

# Soft Matter

Accepted Manuscript



This is an *Accepted Manuscript*, which has been through the Royal Society of Chemistry peer review process and has been accepted for publication.

*Accepted Manuscripts* are published online shortly after acceptance, before technical editing, formatting and proof reading. Using this free service, authors can make their results available to the community, in citable form, before we publish the edited article. We will replace this *Accepted Manuscript* with the edited and formatted *Advance Article* as soon as it is available.

You can find more information about *Accepted Manuscripts* in the [Information for Authors](#).

Please note that technical editing may introduce minor changes to the text and/or graphics, which may alter content. The journal's standard [Terms & Conditions](#) and the [Ethical guidelines](#) still apply. In no event shall the Royal Society of Chemistry be held responsible for any errors or omissions in this *Accepted Manuscript* or any consequences arising from the use of any information it contains.

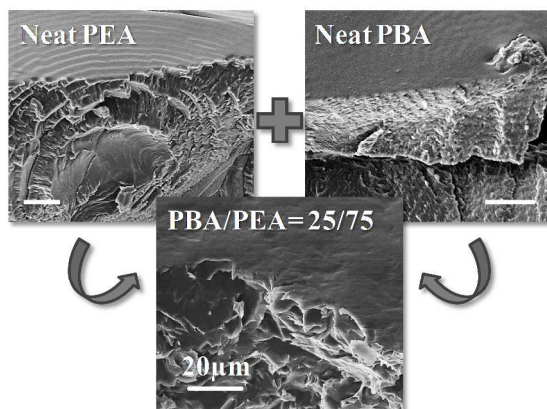
# Intertwining Lamellar Assembly in Porous Spherulites Composed of Two Ring-banded Poly(ethylene adipate) and Poly(butylene adipate)

*Graecia Lugito and Eamor M. Woo\**

Department of Chemical Engineering, National Cheng Kung University, Tainan, 701-01, Taiwan e-mail: emwoo@mail.ncku.edu.tw

## ABSTRACT.

Poly(1,4-butylene adipate) (PBA) and poly(ethylene adipate) (PEA), each with the ability to form ring-banded morphology at same  $T_c$ , were simultaneously crystallized from mixtures of various compositions. Investigations on morphology, phase and thermal behavior were conducted in order to reveal lamellar packing and spherulitic structures in this binary system. As PBA is faster-crystallizing and dominating the crystallization process, PBA is relatively easy to maintain its ordered ring-banded pattern in PBA/PEA blend when PBA is in moderate composition (40 wt-%) or greater. On the other, PEA is much slower-crystallizing and it has to be in extreme majority (PEA > 95 wt-%) in the PBA/PEA mixtures in order to crystallize into ring-banded spherulites of PEA pattern. When PBA composition is between 10 and 40 wt-% in the PBA/PEA blend, simultaneous crystallization of PBA and PEA leads to an interpenetrating morphology with an interwoven bird-nest pattern. Porous structures with crevices, owing to the interpenetrating PBA and PEA lamellae, were resulted in simultaneous crystallization of these two biodegradable polyesters.



## ARTICLE

# Intertwining Lamellar Assembly in Porous Spherulites Composed of Two Ring-banded Poly(ethylene adipate) and Poly(butylene adipate)

Cite this: DOI: 10.1039/x0xx00000x

G. Lugito<sup>a</sup> and E. M. Woo<sup>a</sup>Received 00th January 2012,  
Accepted 00th January 2012

DOI: 10.1039/x0xx00000x

[www.rsc.org/](http://www.rsc.org/)

Poly(1,4-butylene adipate) (PBA) and poly(ethylene adipate) (PEA), each with the ability to form ring-banded morphology at same  $T_c$ , were simultaneously crystallized from mixtures of various compositions. Investigations on morphology, phase and thermal behavior were conducted in order to reveal lamellar packing and spherulitic structures in this binary system. As PBA is faster-crystallizing and dominating the crystallization process, PBA is relatively easy to maintain its ordered ring-banded pattern in PBA/PEA blend when PBA is in moderate composition (40 wt-%) or greater. On the other, PEA is much slower-crystallizing and it has to be in extreme majority (PEA > 95 wt-%) in the PBA/PEA mixtures in order to crystallize into ring-banded spherulites of PEA pattern. When PBA composition is between 10 and 40 wt-% in the PBA/PEA blend, simultaneous crystallization of PBA and PEA leads to an interpenetrating morphology with an interwoven bird-nest pattern. Porous structures with crevices, owing to the interpenetrating PBA and PEA lamellae, were resulted in simultaneous crystallization of these two biodegradable polyesters.

## Introduction

Since last decade, quite many works have been conducted and reported on the blends of two crystallizable polymers<sup>[1–22]</sup> Most of the works are focused on the blends with large melting points difference ( $\Delta T_m$ ) that allow both polymers to crystallize in a stepwise crystallization, where only the high- $T_m$  polymer can crystallize at the first step and the low- $T_m$  polymer crystallize at the following step within a constrained space of the first-step crystals.<sup>[1–17]</sup> Only a few works focus on crystalline/crystalline blends of polymers with simultaneous crystallization, which cover subjects of phase behavior, lamellar assembly, and spherulitic morphology.<sup>[18–22]</sup> Thus, the aim of this study was to further expound effects of two crystal growth on lamellar assembly and spherulitic patterns in blends of two crystallizable polymers with the capability of forming ring-banded spherulites in a common temperature range.

PEA and PBA are both biodegradable semicrystalline

polyesters with similar chemical structure and low melting points (e.g. high biodegradability).<sup>[23]</sup> Due to their biodegradability and biocompatibility, PBA and PEA have been considered as potential materials in drug delivery system.<sup>[24–27]</sup> Hydrophobicity of these polyesters may facilitate the permeation of water into microcapsule structure and as the consequence may also facilitate the drug diffusion rate. They were blended and copolymerized with other polymers in attempt to form porous microsphere/microcapsule.<sup>[24–26]</sup> PBA and PEA are also widely studied in term of their ring-banded morphology and crystal polymorphism.<sup>[28–32]</sup> PEA exhibits double ring-banded spherulites within a narrow crystallization temperature ( $T_c$ ) range of 24 – 34 °C or ringless Maltese-cross spherulites outside the range.<sup>[5,28–32]</sup> PBA exhibits ring-banded patterns within even narrower range of  $T_c$  (ca. 28 – 32 °C), and outside that range, it exhibits ringless Maltese-cross spherulites. In addition to morphology of ring-banded spherulites, PBA also exhibits polymorphic crystal cells (termed  $\alpha$  and  $\beta$ ) in similar temperature range (ca. 27 – 32 °C).<sup>[33–38]</sup> Thermodynamically more stable PBA  $\alpha$ -form, crystallized at higher  $T_c$ , has a monoclinic unit cell with dimensions of  $a = 0.673$  nm,  $b = 0.94$  nm,  $c = 1.420$  nm, and  $\beta = 45.4^\circ$ , whereas kinetically favored PBA  $\beta$ -form, crystallized at lower  $T_c$ , has an orthorhombic unit cell with dimensions  $a = 0.506$  nm,  $b = 0.735$  nm,  $c = 1.467$  nm (fiber axis =  $c$ -axis).<sup>[39–41]</sup> Unlike PBA, which has polymorphic crystal forms depending on its crystallization temperature, PEA

<sup>a</sup> Department of Chemical Engineering, National Cheng Kung University, Tainan, 701-01, Taiwan. E-mail: emwoo@mail.ncku.edu.tw. Electronic Supplementary Information (ESI) available: POM micrographs of neat PBA and neat PEA at various  $T_c$ , POM micrographs of PBA/PEA (10/90 to 50/50) blends crystallized at  $T_c = 28 - 32$  °C, DSC traces for neat PBA melting peaks, and DSC traces for neat PEA melting peaks. See DOI: 10.1039/b000000x/

has only one crystal cell of monoclinic packing, with  $a = 0.547$  nm,  $b = 0.724$  nm,  $c = 1.155$  nm, and a monoclinic angle of  $\alpha = 113.5^\circ$ .<sup>[42]</sup> The fact that both PEA (with monomorphism cell form) and PBA (with polymorphism cell forms) are capable of forming ring-banded spherulites indicates that crystal cell polymorphism is not a necessary condition for ring-banded spherulites. It would be more instructive to examine how spherulite patterns may be constructed from the mixtures of these two polymers when they crystallized together. It should be noted that even though PEA and PBA both attain their respective crystallization kinetics maximum at a similar temperature range, PBA is fast-crystallizing while PEA is slower-crystallizing; thus, in the blend, PBA invariably crystallizes in advance of PEA.

## Experimental

### Materials and preparation

Materials used in this study are as follows. PEA and PBA, low-melting semicrystalline polyesters, were purchased as research-grade materials from Aldrich Co. (USA) with molecular weight equal to 10,000 and 12,000 g/mol, respectively. The molecular weights ( $M_w$ ) were determined by gel permeation chromatography (GPC, Waters 410) using tetrahydrofuran (THF) as the eluent at a flow rate of 1.0 mL/min. Polymers were purified by solution filtration using Teflon (PTFE) syringe filter 0.45  $\mu\text{m}$  and dried in a vacuum oven for 7 days in order to remove all the solvent completely. Neat and blends solution samples were made by dissolving 1 wt-% polymer with various compositions of PBA and PEA into chloroform ( $\text{CHCl}_3$ ) as the solvent. Thin-film samples were prepared by once drip-cast solution on glass slides at 45  $^\circ\text{C}$ , while bulk samples were prepared by repeatedly drip-casting the polymer solutions on flat aluminum pans to stack into thicker films. Solvent in the samples was allowed to evaporate at ambient for 24 hours, before further degassed in a vacuum oven for one week at 40  $^\circ\text{C}$ .

### Apparatus and procedures

Glass transition temperatures ( $T_g$ ) were measured with a differential scanning calorimeter (Perkin-Elmer DSC-7) equipped with a mechanical intracooler and a computer for data acquisition/analysis, liquid nitrogen was used as the cooling media. The other thermal behavior and crystallization kinetics were measured by using DSC Diamond (Perkin-Elmer Corp., USA), equipped with an intra-cooler. During the thermal treatments, a continuous flow rate of nitrogen in the DSC chamber was maintained to prevent sample degradation. For  $T_g$  measurement, samples were first melted at  $T_{max} = 80$   $^\circ\text{C}$  for 2 minutes, then rapidly quenched to  $-120$   $^\circ\text{C}$  and directly reheated to 80  $^\circ\text{C}$  with heating rates of 20 or 40  $^\circ\text{C}/\text{minute}$ .  $T_g$  values were taken as the onset of the second-heating traces. For isothermal crystallization, samples were melted at 80  $^\circ\text{C}$  for 2 minutes to erase the memory effect, then quenched to desire  $T_c$

and had been kept at  $T_c$  until fully crystallized before being reheated to 80  $^\circ\text{C}$  with heating rate of 10  $^\circ\text{C}/\text{minute}$ .

A polarized-light optical microscopy (POM, Nikon Optiphot-2), equipped with a Nikon Digital Sight (DS)-U1 camera control system and a microscopic hot stage (Linkam THMS-600 with T95 temperature programmer), was used to characterize the optical transparency and crystalline morphology of the blends. Observation of spherulitic growth and patterns of neat PBA, PEA, and blend system (either PBA/PEA of various compositions) were performed in the polarized-light microscope (Nikon Optiphot-2, POL). The as-cast neat polymer and blend samples, with thickness ca. 4 – 7  $\mu\text{m}$ , were dried properly before they were examined using POM.

Fractured surfaces of bulk samples were examined and characterized using scanning electron microscopy (FEI Quanta-400F, SEM) for revealing lamellar structure in the fracture and top free surface. Samples were coated with gold vapor deposition using vacuum sputtering (2 mA, 12 x 30 seconds) prior to SEM characterization.

Shimadzu XRD-6000 X-ray diffractometer with copper  $K\alpha$  radiation (at 30 kV and 40 mA) and a monochromatized wavelength of 1.542  $\text{Å}$  was used to determine the crystal structure of neat and PBA/PEA blend. The scanning  $2\theta$  angles were ranging from 10 $^\circ$  to 30 $^\circ$  with a scanning rate of 2 $^\circ/\text{min}$ .

SAXS measurements were performed at beamline BL23A of the National Synchrotron Radiation Research Center (NSRRC), Hsinchu, Taiwan. A monochromatized X-ray radiation source of energy 15 keV and a two-dimensional Pilatus detector were used to collect 2D SAXS patterns. The distance from the sample to the detector was 3255.8 mm. The scattering vector,  $q$  ( $q = 4\pi/\lambda \sin \theta$ ), with scattering angle  $\theta$ , in these patterns was calibrated with silver behenate. After background subtraction and data reduction, 1D SAXS profiles with relative intensity ( $Iq^2$ ) distributions as a function of  $q$  were obtained.

Fourier-transform infrared (FTIR) spectroscopy (Nicolet Magna-560) was used to identify possible intermolecular interaction between PBA and PEA. All spectra were recorded at resolution 4  $\text{cm}^{-1}$  with accumulation of 64 scans. Samples were prepared as cast thin and uniform films from 1 wt-% solution on KBr pellets. The vacuum dried KBr cast samples were thermally treated on the hot stage prior the IR measurement at ambient temperature.

## Results and discussion

### Phase behavior and morphology of PBA/PEA blends

Prior to investigation on their crystalline domains, the phase behavior in mixtures of PBA and PEA of various compositions was first to be proved. Fig. 1 shows thermal analysis and morphology results in confirming the miscibility in PBA/PEA blends: (a) composition-dependent glass transition temperature ( $T_g$ ) and (b) optical microscopy characterization of a representative PBA/PEA = 25/75 blend compositions. The glass

transition temperatures of these two polymers do not differ much; however, shifting of  $T_g$  with respect to blend compositions could still be seen. As shown in Fig. 1a, PBA/PEA blends show a sigmoidal  $T_g$ -composition behavior, which indicates that the interaction and scale of mixing of the blends may differ with respect to the composition.  $T_g$  of the blends could be fitted well using the Kwei equation,<sup>[43]</sup> with the values of parameters  $k$  and  $q$  equal to 0.16 and 46.6, respectively. Stronger interaction is achieved when the composition of PEA is below 60 wt-% (positive  $T_g$  deviation); out of that range of composition, the blends show weaker interaction (negative  $T_g$  deviation).<sup>[43–44]</sup> The optical transparency is also observed in all compositions of the blend, even for 25/75 PBA/PEA blend which clearly shows a unique morphology which completely distinct from other ring-banded or ringless morphology of both neat polymers (Fig. 1b). The as-cast sample was observed under the optical microscope and the top POM graph was collected at room temperature (RT) prior to the heating process of 2 °C/minute to  $T_m$  (80 °C). At  $T_m$ , the OM graph shows a clear and homogeneous phase. After being cooled to RT with the same rate (2 °C/minute), the blend shows a clear POM image without any phase separation could be observed. Thus, by these results, PBA/PEA could be determined as a miscible blend system.

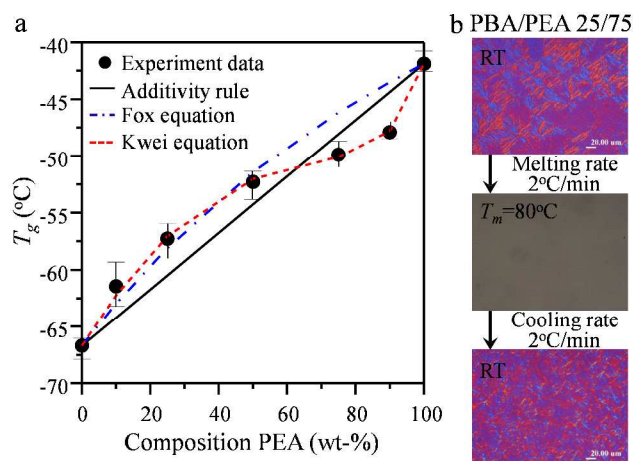


Fig. 1 Thermal analysis and morphology results in confirming the miscibility in PBA/PEA blends: (a) composition-dependent  $T_g$  and (b) optical microscopy characterization of a representative PBA/PEA = 25/75 blend compositions.

Both PBA and PEA show ring-banded morphology within narrow range of  $T_c$  (28 – 32 °C for PBA and 24 – 34 °C for PEA). The complete POM images of neat samples are attached as supporting information S-1. Apparently, there is a common range of  $T_c$  (30 ± 1 °C) where both PEA and PBA show clear and regular ring bands. Patterns of spherulites in PBA/PEA blends of various compositions crystallized in and out of this narrow  $T_c$  range were further probed. It has been discussed previously that the PBA/PEA blend shows melt-miscible behavior in all compositions. However, for brevity, only three compositions of 5/95, 25/75, and 60/40 were selected to expand the morphological behavior of PBA/PEA blends.

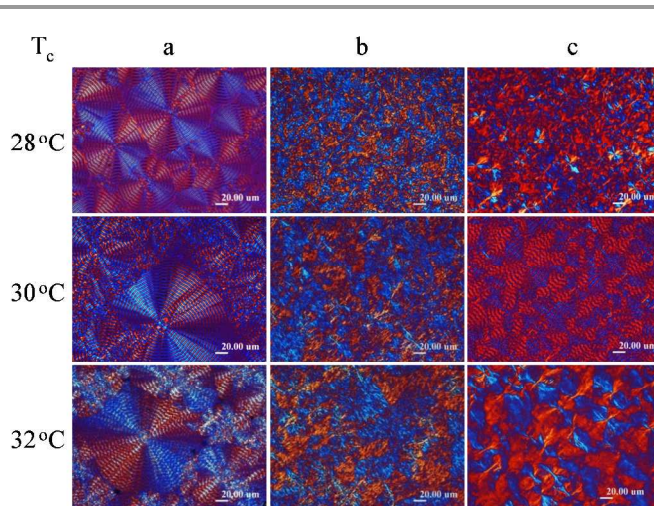


Fig. 2 POM micrographs of PBA/PEA blend with composition of: (a) 5/95, (b) 25/75, and (c) 60/40, crystallized at various  $T_c$  as indicated on the graphs.

Fig. 2 shows POM micrographs of PBA/PEA blend with compositions: (a) 5/95, (b) 25/75, and (c) 60/40, crystallized at various  $T_c$  as indicated on the graphs. As shown in Fig. 2a, the addition of 5 wt-% PBA in 5/95 PBA/PEA blend increases the nucleation density, but decreases both regularity and uniformity of PEA spherulites. Within the same OM-focal area (300 μm × 225 μm) at a same  $T_c$ , there is only 1 or 2 spherulites in neat PEA, while more than 4 large spherulites along with numerous tiny spherulites appear in the 5/95 PBA/PEA blend. As a miscible blend, PBA chains were scattered between PEA chains at the homogeneous melting state. The high crystallization rate of PBA coupled with the weak interaction between PBA and PEA promote PBA nucleation at the first-stage crystallization of this PBA/PEA mixture. However, with low chain density (i.e., low diffusion rate), these PBA crystals could be more hindered to make their own spherulites. The spherulites of lower  $T_c$  are more uniform in size compared to the ones of higher  $T_c$ , indicating that the ability of each component to grow in their own spherulites increases with the increasing of  $T_c$ . Nevertheless, a noticeable disproportion between the center and the later growth part of spherulites indicates PBA may also act as a secondary nucleus for PEA in subsequent crystallization of the mixture. In the other region, PBA dominant, 40 wt-% PEA in 60/40 PBA/PEA blend (Fig. 2c) not only increases the nucleation density, but also reduces the  $T_c$  range of the ring-banded morphology formation of PBA. This blend shows ring bands in spherulites only when it is crystallized at 30 °C, whereas in neat PBA, the ring bands can be observed at  $T_c$  = 29 – 31 °C. In the middle region, 25/75 PBA/PEA blend shows a unique morphology, which is totally different from neat PBA and neat PEA. When crystallized at all  $T_c$  from 28 to 32 °C as shown in Fig. 2b, this blend shows the same morphology of nest-like spherulites, differing only in size (i.e. higher  $T_c$  larger spherulites' size).

Overall, in PBA/PEA blends, the morphologies that similar to those neat polymers are observed when the PEA content is below 60 wt-% (resembling to PBA spherulites) or as high as

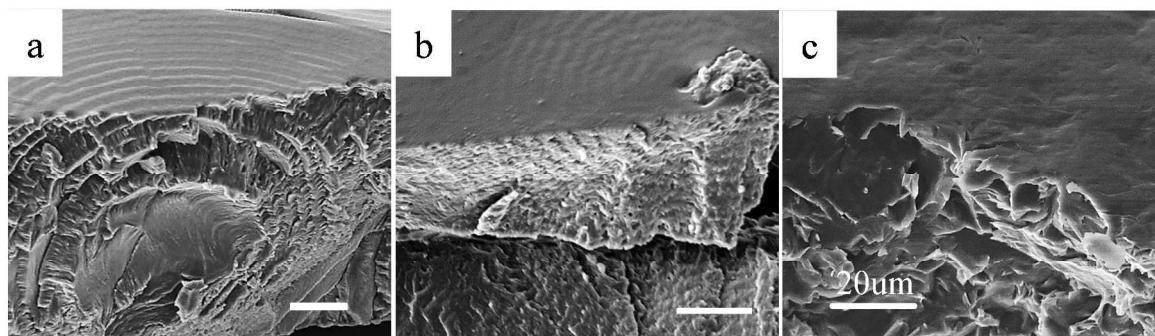


Fig. 3 Detail interior of spherulites formed in (a) neat PEA, (b) neat PBA, and PBA/PEA blend with composition (c) 25/75, crystallized at 30 °C (scale bars = 20 μm).

95 wt-% (resembling to PEA spherulites though surrounded by numerous tiny spherulites). In the intermediate blend compositions, where PEA content is ca. 60 to 90 wt-%, ring bands in spherulites appear to be mutually interfered and become fully extinct from spherulites (POM images are attached as supporting information S-2). The highly intertwining PBA and PEA lamellae significantly disrupt the regularity of banding patterns at these compositions. By comparing the morphology with the interaction strength of the blends (indicated through the composition-dependent  $T_g$  profile), the nest-like morphologies are observed in the blends that show negative  $T_g$  deviation or weak interaction (i.e. 40/60  $\leq$  PBA/PEA < 0/100), except the 5/95 blend.

Interior lamellae and their inner assembled patterns of spherulites in neat and PBA/PEA blend (of various compositions) were further investigated using scanning electron microscope (SEM) to observe the fractured interior surfaces of the samples. Fig. 3 shows the detailed interior of spherulites formed in (a) neat PEA, (b) neat PBA, and blend PBA/PEA with composition (c) 25/75, crystallized at 30 °C. The fracture surface of neat PBA and neat PEA shows a condensed/compact lamellar arrangement. Nevertheless, the blend of those two in 25/75 PBA/PEA composition shows a porous structure with a quite large number of cavities. The uniquely random intertwining lamellar arrangement inside the spherulites could be a plausible reason why PBA/PEA 25/75 blend exhibits a different POM morphology. PBA and PEA, both are capable of aligning their lamellae into orderly patterns of respective ring-banded spherulites when crystallized on its own at this common  $T_c$  (30 °C); however, when blended and simultaneously crystallized, the crystalline lamellae of two different species inevitably impinge on each other, causing flipping, turning, and mutual intertwining of two crystal-plates. Such mutual disruption also leads to disappearance of ring bands in PBA/PEA blend with intermediate compositions (10/90 to 40/60), crystallized at  $T_c = 30$  °C.

Formation of porous lamellar structures induced by crystallization in PLLA/PBA blend with UCST phenomenon has been previously reported.<sup>[16]</sup> Preformed PLLA spherulites at 110 °C act as a growth template of PBA crystallization at ambient temperature. The lamellar re-orientation and volume reduction resulting from the PBA crystallization have been

found as the driving forces of this porous structure formation and the pore size is depended on blend composition. Thus, the interior observation has also been conducted for other PBA/PEA compositions.

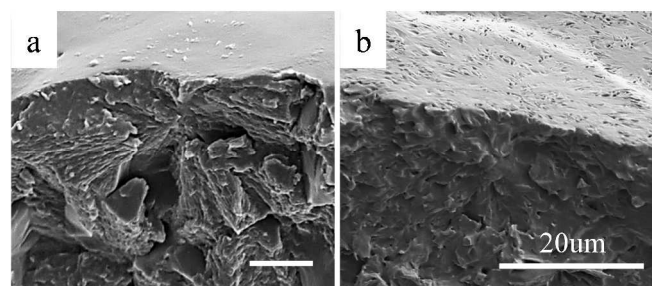


Fig. 4 Detailed interiors showing minor disruption of ring bands in spherulite formed in blend PBA/PEA: (a) 5/95 blend, and (b) 60/40 blend, crystallized at 30 °C (scale bars = 20 μm).

Fig. 4 shows the detailed interiors of spherulites formed in blend PBA/PEA: (a) 5/95 blend and (b) 60/40 blend, all crystallized at 30 °C. The surfaces of those blends still show ring-banded morphology resembling neat PEA and neat PBA, respectively. Although the morphology of most spherulites in PBA/PEA 5/95 blend resembles that of the banded spherulite of neat PEA, cavities are still obviously present in some PBA/PEA spherulites, as shown in Fig. 4a. Mostly in general, the cavities appear in the center and boundaries parts of the spherulites, which might indicate the weakest part (easy to break/rupture) where PBA (minor component) lamellae are located. The 60/40 PBA/PEA blend (Fig. 4b), with a stronger interaction between PBA and PEA, shows much more compact lamellae in the fracture surface, however, cavities with smaller sizes can still be observed. The lamellar intertwining, interpenetration, bending and/or flipping between the PBA and PEA crystals in the blend during crystallization may vary with the composition ratio in the blend and lead to formation of various degrees of microporous-structured spherulites.

#### Thermal behavior in correlation to the morphology

In order to expound the thermal and morphological phenomenon in the blend system, comparisons of DSC and POM results were conducted. POM micrographs along with the

crystallization and melting process were collected simultaneously then direction comparisons of crystallization and melting peaks of samples obtained from DSC were attempted. To minimize the effects of the minute temperature differences, if any, between the microscopic hot stage and DSC heating cell, samples for POM characterization prepared in both apparatus of thermal treatment were compared and temperature of both instruments was maintained to give the minimal possible deviations of temperature effects. The discussions are focused on the blend PBA/PEA crystallized at 30 °C, where

regular ring-banded spherulites could be observed in both neat systems (PBA or PEA). Fig. 5 shows (a) DSC isotherm curves of crystallization, for direct comparison with (b) POM graphs of PBA/PEA blend of various compositions captured at  $T_c = 30$  °C for different time of crystallization as ascribed on the graphs. Prior to the observations, all samples were melted at  $T_{max} = 80$  °C for 2 minutes to erase all prior histories, then quenched to  $T_c = 30$  °C to initiate the isothermal crystallization for  $t = 0$  to the end of crystallization.

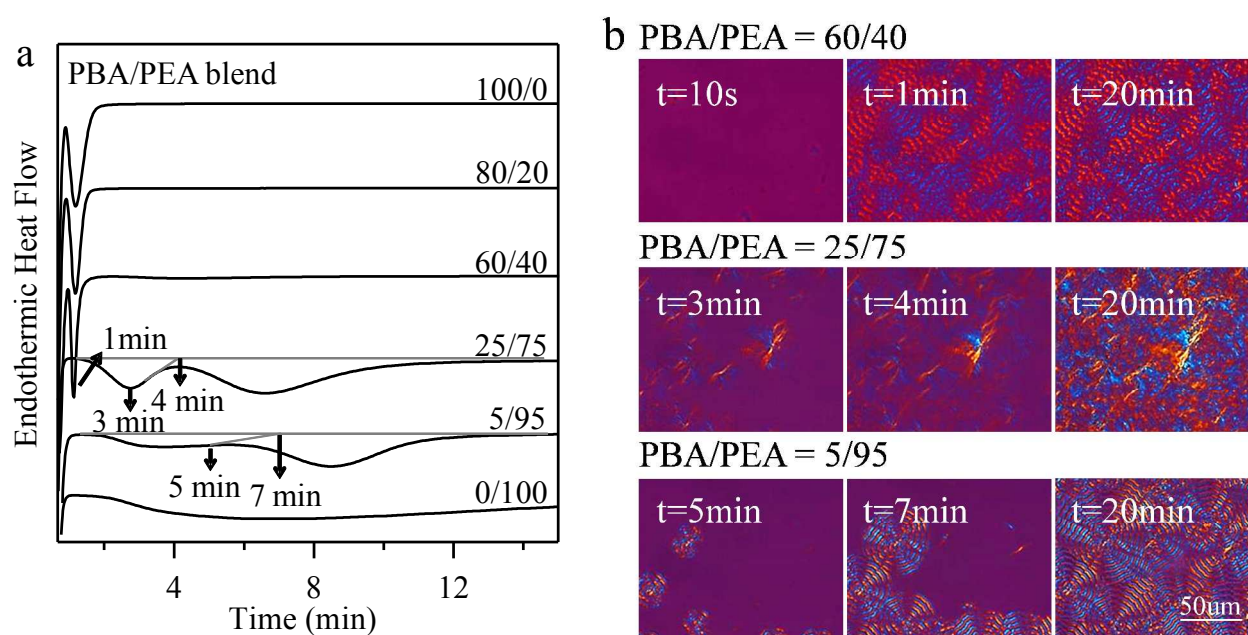


Fig. 5 (a) DSC isotherm curves of crystallization, and (b) POM graphs of PBA/PEA blend of various compositions captured at  $T_c = 30$  °C for different time of crystallization as ascribed on each of the graphs.

The significant difference in the crystallization rates between neat PBA and PEA may be responsible for the appearance of double crystallization peaks (one for PBA and the other for PEA) in DSC run as illustrated in Fig. 5a. The DSC isotherm curves of crystallization show that for low- to medium PEA contents ( $0 < \text{PEA} \leq 40$  wt-%) in PBA/PEA blends, the crystallization exhibits a single exotherm reflecting that the crystallization of these blends is dominated by PBA component. The corresponding POM graphs for morphology of PBA/PEA blend in Fig. 5b show that the crystallized spherulites of PBA/PEA blend composition 60/40 displays distinctly PBA ring bands, with only a little birefringence increment after being crystallized for 20 minutes. These results indicate that the major PBA content is able to draw PEA chains to simultaneously crystallize together in a single stage of crystallization, leaving barely small amount of PEA to crystallize after in secondary crystallization (the amount is too small to be considered as another crystallization peak).

Additional information could be obtained from the correlation between kinetics and morphological evolution. With PEA contents increase to above 40 wt-%, two-steps crystallization of the blends are inevitable, with the primary

crystallization stage being mainly PBA (at shorter time) and secondary stage being PEA (at longer time), forming an intertwining network of lamellae. With increasingly more PEA contents in the blend (75 to 95 wt-%), the dual exotherm peaks are both significantly delayed. The POM graphs of 25/75 blend in Fig. 5b show that the spherulites matrix of a bird-nest-like structure in this blend is completely formed during the first simultaneous crystallization stage of PBA-PEA, and a birefringence increment is seen obviously during the secondary crystallization stage of PEA. These results indicate that the minor PBA content is not sufficient to draw PEA to simultaneously crystallize together in its form (ring-banded spherulite). Nevertheless, at the first-stage period of time, PEA is also able to crystallize; thus, the spherulite matrix is composed of random intertwining lamellae of a bird-nest structure. While for PBA/PEA blend composition 5/95, the minor PBA component in the blend only suffices to crystallize into tiny crystals as nuclei for PEA to further crystallize in later time, and owing to the PBA nucleation occurring during the first crystallization stage, subsequently PEA crystallizes into PEA spherulites of its own kind during the second stage. The mere amount of PBA 5 wt-% in the PBA/PEA (5/95) blend

may not be adequate to simultaneously crystallize with PEA for forming a bird-nest structure; instead, the spherulites in crystallized PBA/PEA (5/95) blend are dominated by the slow-crystallizing PEA to assume the PEA's ring-banded pattern, without intertwining lamellae.

As shown and discussed above, there are two main findings from the real-time comparisons between the morphology and crystallization behavior of PBA/PEA blends. First, it is shown clearly that neat PEA needs much longer time to crystallize than neat PBA at the same  $T_c$ . For the same  $T_c$  (30 °C), PEA needs more than 30 minutes to fully crystallize, while it takes barely two minutes for PBA. Secondly, since the PBA component is more rapidly crystallizable than PEA, it can be expected that PBA takes a dominant role in the crystallization of the PBA/PEA mixtures of most blend compositions. The crystallization isotherms of the PBA/PEA blend of various compositions show that the PBA presence significantly enhances the crystallization rate of PEA; vice versa, the presence of PEA in minor to medium amount influences only little the PBA crystallization.

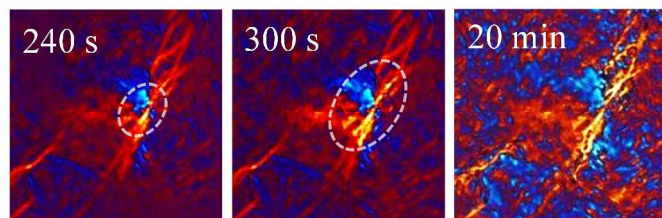


Fig. 6 POM in situ time-evolution graphs of crystal growth of PBA/PEA (25/75) blend crystallized at 30 °C.

Especially of interest is the isothermal crystallization curve for PBA/PEA blend (25/75), where dual exotherm peaks are prominently observed. Fig. 6 shows in situ analysis of POM crystallization period. The figure shows that interpenetration of the later-crystallized PEA indicated by the birefringence increment starts from the center to the edge of PBA-PEA spherulite matrix. This result is different from other reported cases of the crystalline/crystalline blends with two-steps crystallization system where molten species of the component with lower melting temperature (or lower-crystallizing species) are expelled during the crystallization of the component with higher melting temperature (or faster-crystallizing species).<sup>[2–15]</sup> For most intermediate blend compositions, formation of spherulite matrix apparently involves simultaneous crystallization of both PBA and PEA components, and the birefringence enhancement occurs due to epitaxial growth of the remaining slower-crystallizing PEA on the surface of the former spherulite matrix.

Fig. 7 shows an illustration of the crystallization schemes in PBA/PEA blend of intermediate compositions. In these compositions, both PBA and PEA are crystallized together in one step crystallization with two stages crystallization period due to their crystallization rate difference. This condition allows the molten PEA constituent with lower crystallization rate to be remained inside the spherulite matrix, which

primarily formed by the simultaneous crystallization PBA and PEA. The remaining molten PEA constituent then starts to crystallize at the secondary crystallization stage. Cavities observed in the crystallized interiors could likely be formed by the lamellar re-orientation and volume reduction resulting from the secondary crystallization of molten PEA trapped inside the primarily crystallized spherulite matrix.<sup>[16]</sup> Apparently, the crystal arrangement into bird-nest-like lamellae in the crystallized PBA/PEA blend is due to the fact that each of these two polymer components in its own neat form may crystallize into ring-banded corrugated-board layers in 3D spherulites, but differ in their crystallization rates owing to differences in chemical structures.<sup>[30–32,45,46]</sup> The corrugated-board structure of PBA is to be followed by another corrugated-board structure of PEA, leading to interwoven lamellae in 3-D forms. When viewed from the external top surface, the intertwined lamellae in PBA/PEA blend 25/75 appear as a bird-nest pattern (each of the intertwined twigs resembles a crystalline lamella).

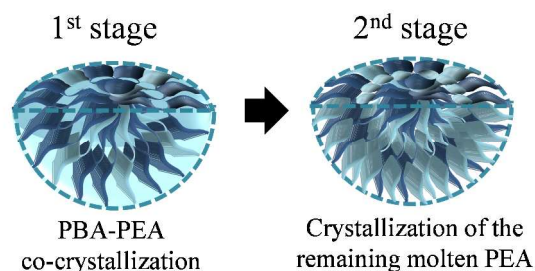


Fig. 7 Illustration of the crystallization schemes in intermediate compositions of PBA/PEA blend system.

Melting behavior of the crystallized PBA/PEA was further analyzed by thermal analysis and compared to reveal the nature of the crystallized lamellae there in the spherulites. Again, for direct comparisons of in-time crystalline morphology and thermal behavior, Fig. 8 shows DSC traces of melting behavior and POM graphs (inset) of PBA/PEA blend with various compositions, formerly melted at  $T_{max} = 80$  °C for 2 minutes then quenched to  $T_c = 30$  °C for full crystallization, before being scanned with melting rate = 10 °C/minute. Numerous melting peaks, up to four peaks and some partially overlapped, are present in the simultaneous crystallization PBA/PEA blends. DSC traces for melting peaks of neat PBA and neat PEA are attached as supporting information S-3 and S-4, respectively. Both neat polymers can exhibit multiple-melting peaks around 42 to 53 °C;<sup>[29–31,34,37,47]</sup> with some peaks overlapping with each other, especially in samples crystallized at 30 °C. However, at temperature 46 °C, almost all PEA crystals in PEA/PBA sample crystallized at 30 °C are melted, while only a small amount of PBA crystals just starts to melt. Thus the morphology observation of the blends was collected at  $T_c$  (30 °C) and at 46 °C. Upon being melted to 46 °C, the spherulite matrix of the blends still remains, but the birefringence of sample darkens. For PBA/PEA blend 5/95, the core regions of spherulites have almost faded completely in birefringence (shown by arrow), leaving the ring-banded part to remain but in very low

birefringence. This result is in agreement with previous reports that the higher melting peak of PEA belongs to the minor part of tangential lamellae which arrange the sheath layer of each band.<sup>[30,31]</sup> There are also some areas (supposedly were encountered by PBA) in the intersection boundaries of the spherulites, indicated by white dash-lines, in which birefringence has almost completely faded. By comparing to the neat PBA (Figure S-3), the DSC traces of PBA/PEA (5/95) blend show no diffraction peaks corresponding to the recrystallized PBA  $\alpha$ -form crystals ( $T_{m4}$ ). The 5 wt-% of PBA in the blend is apparently crystallized in the original  $\alpha$ -form crystal, which has a low melting temperature (lower than 46 °C) with no ability to recrystallize into higher melting-temperature  $\alpha$ -form crystal.<sup>[3,37,47]</sup> Noteworthy to mention here is that similar to crystal lattices in PEA, the  $\alpha$ -form PBA also has a monoclinic unit cell. Thus the investigation to PBA polymorphism in these blends is needed in order to reveal the interaction between PBA and PEA crystals.

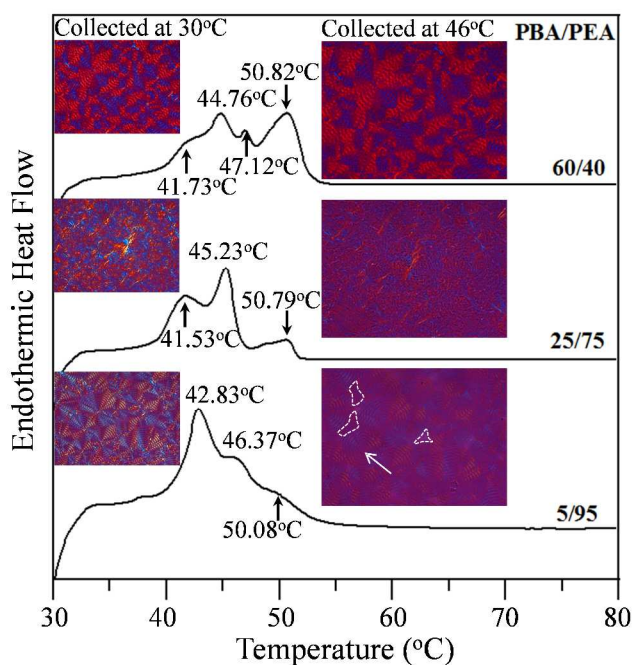


Fig. 8 DSC traces of melting behavior and POM graphs (inset) of PBA / PEA blend with various compositions, formerly melted at  $T_{max} = 80$  °C for 2 minutes then quenched to  $T_c = 30$  °C for full crystallization, before being scanned with melting rate = 10 °C/minute.

### Crystallographic and FTIR characterizations of PBA/PEA blends

The crystal cell structure of nest-like morphology, in comparison to the regular ring-banded patterns, in the PBA/PEA blend was investigated by using X-ray diffractometer. Fig. 9 shows the XRD patterns of neat PBA, PEA, and PBA/PEA blends crystallized at 30 °C as indicated on the graph. The gray dash lines indicate the crystalline peaks of

PEA, the black dash lines indicate the crystalline peaks of  $\alpha$ -form PBA, and the black dot lines indicate the crystalline peaks of PBA  $\beta$ -form. For references, the WAXD data for PBA, PEA, and PBA/PEA blends are listed in Table 1. The values of X-ray diffraction peaks and positions for neat PBA and PEA are consistent with those already known in the literature, from which the values of diffraction peaks for PEA/PBA blend could be compared. By comparing the diffraction peaks of PEA and PBA ( $\alpha$ - and  $\beta$ -forms), there are two overlapped peaks observed, with the first one at  $2\theta = 21.3^\circ$  (which belongs to overlapped PEA and PBA  $\alpha$ -form crystals) and second one at  $2\theta = 24.1^\circ$  (which belongs to overlapped PEA and PBA  $\beta$ -form crystals). The black arrows show the depression fraction of  $\beta$ -form PBA in the blend system. From the X-ray patterns, the  $\alpha$ + $\beta$  polymorphism is only observed in neat PBA and PBA/PEA blend 80/20; for the other blend compositions, only the  $\alpha$ -form PBA is observed. In other words, it is more preferable for PBA in PBA/PEA blend to crystallize in  $\alpha$ -form crystal rather than  $\beta$ -form crystal. This fact is quite expected since PBA  $\alpha$ -form crystal has a monoclinic unit cell which is similar to PEA crystal. The same characteristics are also seen in other miscible blend systems involving PBA.<sup>[3,4,48,49]</sup> The overlapping peaks of (110) PEA and (110) PBA  $\alpha$ -form crystals cause a constructive peak intensity effect in PBA/PEA blend 5/95, resulting in a sharper peak at  $2\theta = 21.3^\circ$  in comparison to neat PEA. It was claimed by Inoue et al.<sup>[50]</sup> that for PEA with high  $M_w$  (same as that used in this study), the intensity of (111) and (020) diffraction peaks is associated with the orientation of lamellae in spherulites, and that the highly oriented spherulites in PEA would exhibit much weaker intensity of (111) peak and (020) shoulder peak diffraction. An earlier study in our laboratory has

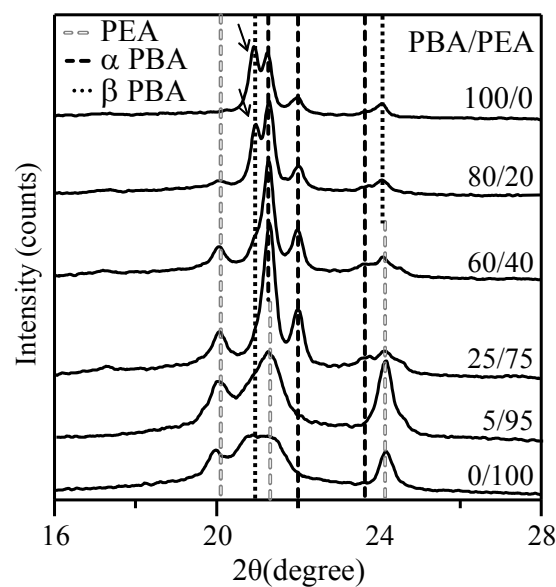


Fig. 9 X-ray patterns of PBA/PEA blends of various compositions crystallized at 30 °C, the corresponding compositions are indicated on the graph.

Table 1 Wide angle X-ray diffraction table of PBA, PEA, and their blends.

Crystal 2θ (°)/plane	PBA/PEA blend composition					
	100/0	80/20	60/40	25/75	5/95	0/100
PBA α-form						
21.3°/(110)	√	√	√	√	√	–
22.0°/(020)	√	√	√	√	√	–
23.6°/(021)	√	√	√	√	–	–
PBA β-form						
20.9°/(110)	√	√	–	–	–	–
24.1°/(020)	√	√	–	–	–	–
PEA						
20.0°/(111)	–	√	√	√	√	√
21.3°/(110)	–	√	√	√	√	√
24.1°/(020)	–	√	√	√	√	√

also pointed out that, instead of using oriented PEA spherulites as shown by Inoue, ring-banded PEA spherulites (crystallized at  $T_c = 28$  °C) also exhibits much lower (111) WAXD diffraction but slightly sharper (020) diffraction intensity.<sup>[30–32]</sup> Such evidence indicates that the cilia-like crystals (straight fibrous lamellae) in the sheath layer of the corrugated-board and ring-band structure may be highly oriented in a uniform direction in the PEA samples exhibiting such corrugate-board lamellae, where tangential lamellae and radial lamellae are collectively packed into 3-D spheroid ring bands.<sup>[32]</sup> Such features are absent in the blends with bird-nest-like patterns.

The WAXD results suggest that after being blended together, the crystal cell structure of PBA and PEA remain the same, suggesting that they are crystallized in their own lattices and individual lamellae. However, these PBA and PEA lamellae can yet intertwine together to form a spherulite with noticeable micro-cavities owing to lamellae impingement and/or intertwining.

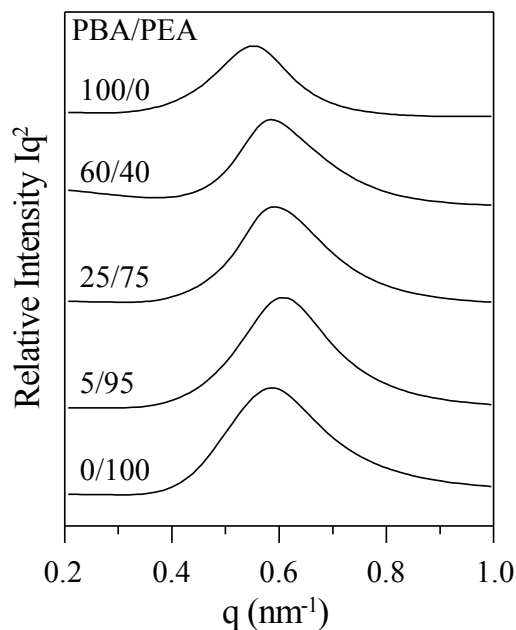


Fig. 10 Lorentz-corrected SAXS profiles of PBA/PEA blends of various compositions crystallized at 30 °C, the corresponding compositions are indicated on the graph.

In addition to the WAXD result as earlier discussed, to evaluate the variation of lamellae thickness in the PBA/PEA blend, small-angle X-ray scattering (SAXS) was performed. Fig. 10 shows Lorentz-corrected SAXS profiles of PBA/PEA blends of various compositions all crystallized at 30°C. Long-periods of each blend composition were calculated from the Bragg's law [long-period ( $L$ ) =  $2\pi/q_{max}$ ]. Neat PEA shows higher  $q$  values in comparison to neat PBA, meaning that PEA has a shorter  $L$ . Interestingly, the  $q$  values of the PBA/PEA blends are higher than those of the two neat polymers. The

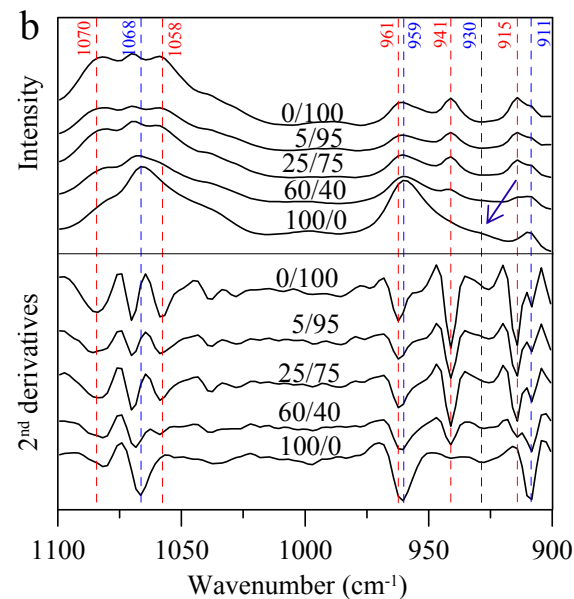
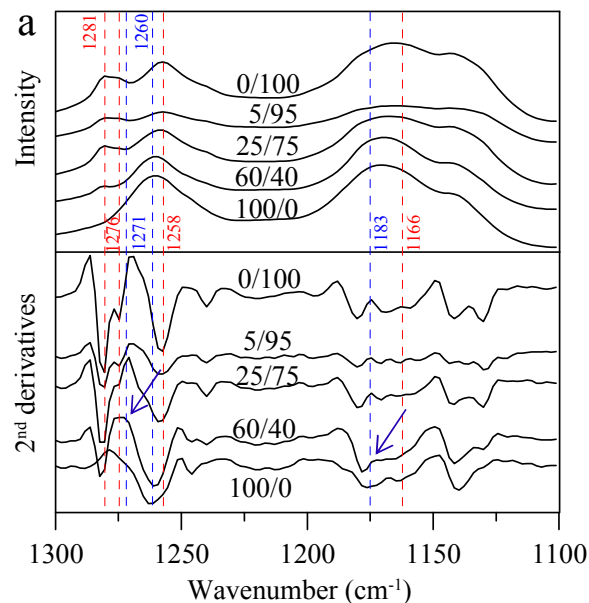


Fig. 11 IR spectra and second derivatives of PBA/PEA blends crystallized at  $T_c = 30$  °C with compositions as indicated on traces [arrow indicates the wavenumbers for which β-PBA can be distinguished from α-PBA].

highest  $q$  value is found in the 5/95 blend, and similar  $q$  values are found in the 25/75 and 60/40 PBA/PEA blends. These SAXS results indicate that simultaneous crystallization of both polymers in the blends indeed confines the growth space of each polymer. In addition, the half-height-full-width of the Lorentz-corrected SAXS profiles representing the first-order Bragg peak were also analyzed to reveal the degree of periodic order of neat PBA, PEA, in comparison to their blend of several compositions. The basic correlation is that the width of the SAXS diffraction curves increases as the degree of the periodic order of crystals decreases, i.e., imperfections would lead to a broadening of the SAXS peaks. However, by comparing the neat polymers with the PBA/PEA blend, the half-height-full-width values of the blend are roughly in between those of neat PBA and PEA. Thus, the lamellar nanostructures in the spherulites of the PBA/PEA blend do not show any significant imperfections, although the growth of the lamellae is reduced.

In order to assess the molecular interactions in the PBA/PEA blend, FTIR characterization of the PBA/PEA blend samples was conducted. The IR characterization was focused on the range of wavenumbers 900–1500  $\text{cm}^{-1}$ , which is known to be more sensitive to crystallization and crystal melting of aliphatic polyesters.<sup>[50–52]</sup> Fig. 11 shows IR spectra of PBA/PEA blend with compositions as indicated. Samples were crystallized at  $T_c = 30$  °C prior the IR characterization, which was conducted at room temperature. A previous work by Yang, et al.<sup>[51]</sup> have reported that the FTIR spectrum of the  $\alpha$ -crystal of PBA differs only in following wavenumbers: 1485, 1271, 1183, and 930  $\text{cm}^{-1}$  from those of the  $\beta$ -crystal. At wavenumber 1485  $\text{cm}^{-1}$  [corresponding to  $\text{CH}_2$  bending], the IR peak of  $\beta$ -form PBA overlaps with some of the absorbance peaks of PEA. By referring to the other three peak wavenumbers, there is no  $\beta$ -form PBA formed in the blend system with PBA composition equals to 60 wt-% or less. This IR result clearly supports the X-ray diffraction data discussed earlier, indicating that PBA in PBA/PEA blend system tends to be crystallized in the  $\alpha$ -form crystal due to the compatibility of PBA  $\alpha$ -form crystal cell with the PEA crystal cell. However, the IR result shows that there are no specifically strong interactions between the PBA and PEA molecular chains, even though they form a mutually homogeneous mixture. This result might be the answer why porous structures are observed in the fracture surface of the blends, even for 60/40 blend which shows stronger interaction between PBA and PEA.

## Conclusions

Two biodegradable aliphatic polyesters, PBA and PEA, both capable of forming ring-banded spherulite when crystallized at a narrow range of  $T_c$  (29 – 31°C) but with different crystallization rates, were blended for probing the lamellar structure in their crystallized spherulites. Simultaneous crystallization was conducted at  $T_c = 30$  °C, as it was the temperature at which both neat PEA and PBA polymers were able to crystallize into ring-banded spherulites. In PEA/PBA blend, ring-band patterns were either preserved or disrupted

into an interwoven bird-nest-like with porous structure, depending on compositions. How two ring-banded polymers (PEA, PBA) in a mixture state were able to simultaneously crystallize into a porous structure by maintaining original banding patterns has been explained.

In the PBA/PEA blend, it is relatively easy for the faster-crystallizing PBA to maintain its ring-banded structure in the PBA/PEA blend. In blends, as long as PBA is higher than 40 wt-% in compositions, the faster-crystallizing PBA predominantly forms the ring-banded spherulite matrix upon crystallization while most of the slower-crystallizing PEA chains are still in a molten state and tend to be segregated out to be located in PBA interlamellae. On the other hand, for the slower-crystallizing PEA to maintain its ring banded patterns in PBA/PEA blend, PEA has to be extremely high (95 wt-% or higher) contents in the blend. Only in this extremely high PEA and very low PBA content (i.e., 5/95 PBA/PEA), PBA exerts a minimum effect and only suffices to crystallize into tiny crystals as nuclei for PEA to further crystallize during the early-stage crystallization, subsequently, the majority PEA crystallizes into ring-banded spherulites of its own kind. However, except for these two extreme cases, in the intermediate PBA/PEA blend compositions, PEA has the ability to simultaneously crystallize with PBA in forming a bird-nest-like spherulites with porous structure as a result of interpenetration and re-orientations of PBA and PEA lamellae. The corrugated-board structure of PBA is to be followed by another corrugated-board structure of PEA, leading to interwoven lamellae in 3-D forms observed from bulk fractured interiors. The interaction between PBA and PEA along with the composition ratio in the blend are supposed to be the driving force of such porous structure formation.

## Acknowledgements

This work has been financially supported by a basic research grant (NSC 102-2221-E-006-268-MY3) for three consecutive years from Taiwan's National Science Council (NSC), now Ministry of Science and Technology (MOST). This research was also partially supported by the Ministry of Education, Taiwan, R. O. C., in aim for the Top-University Project to National Cheng Kung University (NCKU).

SAXS measurements and analyses were performed at beamline BL23A of the National Synchrotron Radiation Research Center (NSRRC), Hsinchu, Taiwan, with professional helps provided from Professor Ya-Sen Sun and Mr. Wei-Cheng Lin of Department of Chemical and Materials Engineering, National Central University, to which the authors would like to express their sincerest grates.

## References

- [1] J. Liu and B. J. Jungnickel, *J. Polym. Sci. Part B: Polym. Phys.* 2007, **111**, 1917–1931.
- [2] H. Wang, Z. Gan, J. M. Schultz and S. Yan, *Polymer* 2008, **49**, 2342–2353.

- [3] J. Yang, P. Pan, L. Hua, Y. Xie, T. Dong, B. Zhu, Y. Inoue and X. Feng, *Polymer* 2011, **52**, 3460–3468.
- [4] J. Yang, P. Pan, L. Hua, B. Zhu, T. Dong and Y. Inoue, *Macromolecules* 2010, **43**, 8610–8618.
- [5] T. Wang, H. Wang, H. Li, Z. Gan and S. Yan, *Phys. Chem. Chem. Phys.* 2009, **11**, 1619–1627.
- [6] Z. Qiu, T. Ikehara and T. Nishia, *Polymer* 2003, **44**, 2799–2806.
- [7] Y. He, B. Zhu, W. H. Kai and Y. Inoue, *Macromolecules* 2004, **37**, 8050–8056.
- [8] H. Wang, J. M. Schultz and S. Yan, *Polymer* 2007, **48**, 3530–3539.
- [9] P. Pan, L. Zhao, J. Yang and Y. Inoue, *Macromol. Mater. Eng.* 2013, **298**, 201–209.
- [10] Y. He, B. Zhu, W. H. Kai and Y. Inoue, *Macromolecules* 2004, **37**, 3337–3345.
- [11] S. He and J. Liu, *Polym. J.* 2007, **39**, 537–542.
- [12] T. Wang, H. Li, F. Wang, J. M. Schultz and S. Yan, *Polym. Chem.* 2011, **2**, 1688–1698.
- [13] H. J. Chiu, H. L. Chen and J. S. Lin, *Polymer* 2001, **42**, 5749–5754.
- [14] J. Liu and B. J. Jungnickel, *J. Polym. Sci. Part B: Polym. Phys.* 2003, **41**, 873–882.
- [15] J. Liu and B. J. Jungnickel, *J. Polym. Sci. Part B: Polym. Phys.* 2004, **42**, 974–985.
- [16] S. Nurkhamidah and E. M. Woo, *Macromolecules* 2012, **45**, 3094–3103.
- [17] Z. He, L. Liang and C. C. Han, *Macromolecules* 2013, **46**, 8264–8274.
- [18] Z. Qiu, T. Ikehara and T. Nishia, *Macromolecules* 2002, **35**, 8251–8254.
- [19] J. Lu, Z. Qiu and W. Yang, *Macromolecules* 2008, **41**, 141–148.
- [20] S. Hirano, Y. Nishikawa, Y. Terada, T. Ikehara and T. Nishi, *Polym. J.* 2002, **34**, 85–88.
- [21] T. Ikehara, H. Kurihara, Z. Qiu, and T. Nishi, *Macromolecules* 2007, **40**, 8726–8730.
- [22] J. B. Zeng, Q. Y. Zhu, Y. D. Li, Z. C. Qiu and Y. Z. Wang, *J. Phys. Chem. B* 2010, **114**, 14827–14833.
- [23] Y. Tokiwa, B. Calabia, C. Ugwu and S. Aiba, *Int. J. Mol. Sci.* 2009, **10**, 3722–3742.
- [24] T. W. Atkins, *J. Biomater. Sci.* 1997, **8**, 833–845.
- [25] T. W. Atkins, *Biomaterials* 1997, **18**, 173–180.
- [26] C. T. Brunner, E. T. Baran, E. D. Pinho, R. L. Reis and N. M. Neves, *Colloid Surface B* 2011, **84**, 498–507.
- [27] X. Q. Shi, H. Ito and T. Kikutani, *Polymer* 2005, **46**, 11442–11450.
- [28] E. Murayama, *Optical properties of ringed spherulites*. 2002.
- [29] E. M. Woo, P. L. Wu, M. C. Wu and K. C. Yan, *Macromol. Chem. Phys.* 2006, **207**, 2232–2243.
- [30] E. M. Woo, L. Y. Wang and S. Nurkhamidah, *Macromolecules*, 2012, **45**, 1375–1383.
- [31] G. Lugito and E. M. Woo, *Colloid. Polym. Sci.* 2013, **291**, 817–826.
- [32] G. Lugito and E. M. Woo, *Cryst. Growth Des.* 2014, **14**, 4929–4936.
- [33] Z. Gan, H. Abe and Y. Doi *Macromol. Chem. Phys.* 2002, **203**, 2369–2374.
- [34] Z. Gan, K. Kuwabara, H. Abe, T. Iwata and Y. Doi, *Biomacromolecules* 2004, **5**, 371–378.
- [35] Z. Gan, K. Kuwabara, H. Abe, T. Iwata, Y. Doi, *Polym. Degrad. Stab.* 2005, **87**, 191–199.
- [36] M. C. Wu and E. M. Woo, *Polym. Int.* 2005, **54**, 1681–1688.
- [37] E. M. Woo, K. C. Yen and M. C. Wu, *J. Polym. Sci. Part B: Polym. Phys.* 2008, **46**, 892–899.
- [38] J. Liu, H. M. Ye, J. Xu, B. H. Guo, *Polymer* 2011, **52**, 4619–4630.
- [39] R. Minke and J. Blackwell, *J. Macromol. Sci.* 1979, **B18**, 407–417.
- [40] R. Minke and J. Blackwell, *J. Macromol. Sci.* 1980, **B18**, 233–255.
- [41] E. Pouget, A. Almontassir, M. T. Casas and J. Puiggali, *Macromolecules* 2003, **36**, 698–705.
- [42] S. Y. Hobbs and F. W. Hobbs, Jr. *J. Polym. Sci. Part A-2: Polym. Phys.* 1969, **7**, 1119–1121.
- [43] T. K. Kwei, E. M. Pearce, J. R. Pennacchia and M. Charton, *Macromolecules* 1987, **20**, 1174–1176.
- [44] Y. He, B. Zhu and Y. Inoue, *Prog. Polym. Sci.* 2004, **29**, 1021–1051.
- [45] A. Frömsdorf, E. M. Woo, L. T. Lee, Y. F. Chen and S. Förster, *Macromol. Rapid Commun.* 2008, **29**, 1322–1328.
- [46] A. Meyer, K. C. Yen, S. H. Li, S. Förster and E. M. Woo, *Ind. Eng. Chem. Res.* 2010, **49**, 12084–12092.
- [47] E. M. Woo and M. C. Wu, *J. Polym. Sci. Part B: Polym. Phys.* 2005, **43**, 1662–1672.
- [48] L. Y. Wang, G. Lugito, E. M. Woo and Y. H. Wang, *Polymer* 2012, **53**, 3815–3826.
- [49] G. Lugito and E. M. Woo, *Macromol. Chem. Phys.* 2012, **213**, 2228–2237.
- [50] J. Yang, P. Pan, T. Dong and Y. Inoue, *Polymer* 2010, **51**, 807–815.
- [51] J. Yang, Z. G. Li, P. Pan, B. Zhu, T. Dong and Y. Inoue, *J. Polym. Sci. Part B: Polym. Phys.* 2009, **47**, 1997–2007.
- [52] C. Yan, Y. Zhang, Y. Hu, Y. Ozaki, D. Shen, Z. Gan, S. Yan and I. Takahashi, *J. Phys. Chem. B* 2008, **112**, 3311–3314.